HHS Public Access

Author manuscript

J Magn Reson Imaging. Author manuscript; available in PMC 2017 February 01.

Published in final edited form as:

J Magn Reson Imaging. 2016 February ; 43(2): 364–372. doi:10.1002/jmri.25003.

Noncontrast MR Angiography (MRA) of Infragenual Arteries Using Flow-Sensitive Dephasing (FSD)-Prepared Steady-State Free Precession (SSFP) at 3.0T: Comparison with Contrast-Enhanced MRA

Nan Zhang, MD[1], **Zhaoyang Fan, PHD**[2], **Nan Luo, MD**[1], **Xiaoming Bi, PHD**[3], **Yike Zhao, MD**[1], **Jing An, PHD**[4], **Jiayi Liu, MD**[1,*], **Zhong Chen, PHD**[5], **Zhanming Fan, PHD**[1], and **Debiao Li, PHD**[2]

[1]Department of Radiology, Beijing Anzhen Hospital, Capital Medical University, Chaoyang District Anzhen Road 2nd, Beijing 100029, China

[2]Biomedical Imaging Research Institute, Cedars-Sinai Medical Center, Los Angeles, California, USA

[3]Siemens Medical Solutions USA, Inc. Chicago, Illinois, USA

[4]Siemens Healthcare, China, MR Collaborations NE Asia, Beijing, China

[5]Department of Vascular Surgery, Beijing Anzhen Hospital, Capital Medical University, Chaoyang District Anzhen Road 2nd, Beijing 100029, China

Abstract

Purpose—To evaluate the feasibility and diagnostic performance of flow-sensitive dephasing (FSD)-prepared steady-state free precession (SSFP) MR angiography (MRA) for imaging infragenual arteries at 3.0T, with contrast enhanced MR angiography (CE MRA) as reference.

Materials And Methods—Twenty consecutive patients with suspicion of lower extremity arterial disease undergoing routine CE MRA were recruited. FSD MRA was performed at calf before CE MRA. Image quality and stenosis degree of infragenual arteries from both techniques were independently evaluated and compared. Six patients in this study underwent DSA examination.

Results—Three undiagnostic segments were excluded with severe venous contamination in CE MRA. A total of 197 calf arterial segments images were analyzed. No significant difference existed in the relative signal intensity (rSI) of arterial segments between FSD MRA and CE MRA techniques (0.92±0.09 vs. 0.93±0.05; P=0.207). However, the subjective image quality score was slightly higher in FSD MRA (3.66±0.81 vs. 3.49±0.87; P=0.050). With CE MRA images as reference standard, slight overestimation existed in FSD MRA (2.19±1.24 vs. 2.09±1.18; P=0.019), with total agreement of 84.3% on the basis of all arterial segments. The sensitivity, specificity, NPV, and PPV of FSD MRA was 96.4%, 93.0%, 98.5%, and 84.1%. No significant

[*]Corresponding to: Jiayi Liu, PHD, Department of Radiology, Beijing Anzhen Hospital, Capital Medical University, Chaoyang District Anzhen Road 2nd, Beijing 100029, China. Tel: +86-13671198400, ljy76519@163.com.

difference in the stenosis degree score was detected between MRA (FSD MRA and CE MRA) and DSA ($P > 0.05$).

Conclusion—FSD MRA performed on at 3.0Twithout the use of contrast medium provides diagnostic images allowing for arterial stenosis assessment of calf arteries that was highly comparable with CE MRA. Moreover, venous contamination was less problematic with FSD MRA.

Keywords

noncontrast MR angiography; peripheral vascular disease; flow-sensitive dephasing; steady-state free precession

INTRODUCTION

In recent years, peripheral artery disease (PAD) has become a global problem (1). Symptoms including intermittent claudication, rest pain and even gangrene adversely affect quality of life for patients suffering from PAD. Contrast-enhanced MR angiography (CE MRA) was previously shown to be a useful method to diagnose anatomic location and degree of stenosis of PAD, especially for the candidates of endovascular intervention therapy (2). However, its application in patients with renal insufficiency is limited due to the risk of gadolinium-based agent derived nephrogenic systemic fibrosis (NSF) (3,4). Therefore, a noncontrast MRA (NC MRA) method is highly desirable (5).

Time-of-flight and phase-contrast are two original NC MRA techniques, but not widely accepted for imaging peripheral arteries, primarily due to the limited spatial coverage (or time inefficiency) as well as well-known flow artifacts associated with complex flow (5). Recently, a group of NC MRA techniques, such as fast spin-echo based fresh blood imaging (FBI) methods (6), quiescent interval single-shot (QISS) (7,8), and balanced steady-state free precession (SSFP) using flow-sensitive dephasing (FSD) magnetization preparation (9) have been developed as an alternative to CE MRA for peripheral MRA. Among them, FSD MRA provides several unique features including high arterial blood SNR and blood-tissue CNR, isotropic sub-millimeter spatial resolution, and flexible FSD module to suppress flow in different directions and with different speed.

The FSD MRA method exploits the arterial pulsatility and introvoxel spin dephasing effect to selectively depict arterial flow. The similar idea dates back to 1980s by Wedeen et al (10) and Meuli et al (11). In brief, two consecutive ECG-triggered 3D balanced SSFP acquisitions are acquired in one scan. The dark-artery measurement is collected during systole exploiting the marked velocity difference between arterial and venous flows. An optimal FSD preparation is employed to intravoxelly dephase the arterial blood spins while having little effect on venous blood and static tissues. The bright-artery measurement is acquired with a zero-gradient-strength FSD preparation (i.e. T2 preparation) during diastole when arterial flow is substantially slow and thus retains high signal intensity on balanced SSFP images. Magnitude subtraction of the two measurements allows the visualization of arteries with dramatically suppressed background and venous signals.

Previous clinical studies evaluating the performance of FSD MRA of the distal lower extremities have focused on 1.5T, showing diagnostic accuracy highly comparable to CE MRA (9,12–14). However, such success may not directly translate to 3.0T mainly due to the balanced SSFP's susceptibility to off-resonance artifacts. The aim of this study was to evaluate the feasibility of FSD MRA for infragenual arteries at 3.0T with CE MRA and digital subtraction angiography (DSA) serving as the standard of reference.

MATERIALS AND METHODS

This prospective study was approved by local ethics committee. Informed consent was obtained from all patients before study enrolment.

From July 2014 to October 2014, 20 patients (15 men, 5 women; mean age 59.61±18.25 years; range 14–84 years) (Table 1) with suspicious PAD at the lower extremities referred for routine lower extremity CE MRA were consecutively enrolled. None of the patients had severe renal failure (estimated glomerular filtration rate (eGFR) ≥30 ml/min/1.73 m^2).

Following the MR examination, six of the 20 subjects were subsequently determined to receive interventional revascularization procedures for stenting and thus they had digital subtraction angiography (DSA) available as gold standard in this work.

MRA exams were performed on a 3.0T MR (Verio, Siemens Healthcare, Erlangen, Germany). Patients were placed with supine position, feet first in the scanner. A 6-element body matrix coil and a 24-element peripheral angiography matrix coil combined with the spine coil were used for signal reception. The ECG signal was monitored with the MRI ECG system during the exam, and used for ECG-triggering. FSD MRA was performed first at the calf station. A three-station protocol of CE MRA followed immediately.

FSD MRA

After a tri-plane localization scan, a 2D transverse phase contrast sequence above the popliteal trifurcation was used for detecting the systolic and diastolic phase for ECG triggering (Figure 1). Encoding velocity = 100 cm/s. After shimming, an ECG-triggered, FSD-prepared 2D segmented bSSFP sequence for first-order gradient moment (m1) scout image (as described in (15)) was performed at the same plane as in the phase contrast scan. Eleven measurements were collected during one scan with starting m1=5 mT·ms^2/m and step size= 5 mT·ms^2/m. The scout images were visually assessed and optimal m1 was chosen for the following 3D FSD MRA sequence to ensure adequate blood suppression in the artery lumen (Figure 2).

FSD MRA (9) was performed using the systolic and diastolic delay times and optimal m1 value determined from the scout scan. Bilateral knees and calves, including the popliteal arteries, anterior and posterior tibial arteries, tibioperoneal trunk, and perennial arteries, were covered by an oblique coronal volume (13). Parameters for imaging included: TE/TR = 1.9/450 ms, receiver bandwidth = 965 Hz/pixel, FOV = 400 × 320 mm^2, acquisition matrix = 288×294, slice thickness = 1.0 mm, 56 slices per slab, flip angle = 53°, three shots per

partition (60 lines per cardiac cycle), GRAPPA acceleration factor = 2 in the phase-encoding direction, acquisition time=4–5 min (depending on heart rate).

CE MRA

3D gradient-echo (fast low-angle shot (FLASH)) sequence was used to acquire three stations in coronal orientation before and after contrast medium administration. K-space was filled with a central first approach, and time-to-center = 1 s. TR/TE = 3.2/1.2 ms, receiver bandwidth = 698 Hz/pixel, FOV = 350×400 mm^2, acquisition matrix = 369×448, slice thickness = 0.9 mm, 104 slices per slab, flip angle = 25°, acquisition time = 63 s (each sequence for 19 s with extra 6 s for two table movements).

For all examinations, a 2D gradient-echo sequence was used to monitor the arrival of contrast agent at abdominal aorta. Single dose (0.1 mmol/kg bodyweight) Magnevist (Bayer Schering Pharma AG, Germany) was injected through median cubital vein at a rate of 2.0 mL/s followed by a 20 mL saline flush injected at the same rate. The amount of contrast was limited to 20ml, in case a patient's bodyweight dictated more.

Image Analysis

Images of all examination were evaluated separately by two radiologic readers with more than 5 years working experience in cardiovascular imaging (N.Z. 5 years and J.L. 10 years). The name, date and sequence of cases were concealed to the readers. Image post-processing and evaluation were performed with a Siemens workstation (SyngoMMWP VE40A, Siemens Med Service Software). Maximum intensity projection (MIP) images of the subtracted data sets were created for evaluation. Disagreement was resolved by consensus.

Five arterial segments (the popliteal artery, the tibioperoneal trunk, the anterior tibial artery, the posterior tibial artery, and the perennial artery) were evaluated for each calf. All the images were assessed for image quality and stenosis degree.

Image Quality Assessment

Signal-to-noise ratio (SNR) and contrast-to-noise ratio (CNR) were not calculated because of the parallel imaging induced heterogeneous noise distribution (16). Signal intensity (SI) was measured at the center of normal portion of the arterial segment with 0.08–0.11 cm^2 circular regions of interest (ROI). Signal intensity of surrounding soft tissue was measured from the muscle adjacent to the artery portions used before with a ~1.0-cm^2 ROI. Relative signal intensity (rSI) defined below was determined for each arterial segment for quantitative assessment of the relative contrast (16):

$$rSI=\frac{\text{Artery SI}-\text{Muscle SI}}{\text{Artery SI}+\text{Muscle SI}}$$

A 4-point scale was used to measure the image quality of each segment:1, non-diagnostic due to poor delineation of major arteries or severe venous contamination; 2, fair delineation of major arteries or some venous contamination; 3, good delineation of major arteries or minor venous contamination; 4, excellent delineation of major arteries and no venous

contamination. (9). The segments scored 2 to 4 were deemed diagnostic. Image quality was not evaluated on occlusive segments because of invisible lumen of the segments (16). The lowest score was used for patient's basis analysis.

Arterial Stenosis Assessment

Arterial stenosis degree was evaluated from MIP images. A 4-point scale evaluation criteria (1. normal; 2. luminal narrowing <50%; 3. luminal narrowing ≥50%; 4. occluded) was used to evaluate the stenosis degree for each arterial segment. If there was more than one stenosis lesion present in one segment, the most severe lesion was used to describe the stenosis degree of the arterial segment (13) and patient's basis analysis. The agreement of stenosis scores between FSD MRA and CE MRA images was calculated.

Arterial segments scored 3 and 4 (i.e. luminal narrowing ≥50% or occluded) were considered as significant stenosis segments. Using CE MRA images as a reference standard, the diagnostic sensitivity, specificity, negative predictive value (NPV) and positive predictive value (PPV) of FSD MRA in terms of the detection of significant stenosis was evaluated.

Interventional Digital Subtraction Angiography (DSA)

Six patients in our study underwent conventional intra-arterial DSA studies by using a trans-femoral artery approach within one week after MR examination. Selective popliteal artery catheterization and infragenual arteries angiography were performed on a digital angiography unit (Allura Xper FD10, Philips medical systems, Netherlands). Arterial stenosis degree with the same 4-point scale was assessed for each arterial segment at calf station in DSA images. The difference of arterial stenosis degree assessment between MRA (FSD MRA and CE MRA) and DSA was evaluated. Regarding ≥50% as significant stenosis, diagnostic sensitivity, specificity, NPV and PPV of MRA (FSD MRA and CE MRA) in terms of the detection of significant stenosis was evaluated.

Statistical Analysis

The statistical analysis was calculated on a per-segment and per-patient basis, respectively, using a statistical software package (SPSS 19.0, SPSS Inc., an IBM company, USA). Continuous numerical variables were expressed as mean ± SD. Because the continuous variables were normally distributed (according to Kolmogorov–Smirnoff test results), difference of arterial segments' rSI between FSD MRA group and CE MRA group was calculated with paired t-test. Discrete variables' (image quality score and arterial stenosis degree score) differences between FSD MRA group and CE MRA group were compared with Wilcox signed rank test. Also Wilcox signed rank test was used to detect the difference of arterial stenosis degree assessment between MRA and DSA. Cohen κ statistic was used for consistency between different observers in image quality and arterial stenosis assessment. Consistencies with kappa value no less than 0.75 were deemed good. A two-tailed P value of 0.05 or less indicated a statistically significant difference.

RESULTS

After excluding the area contaminated by off-resonance or banding artifacts caused by B_0 inhomogeneity, the effective FOV for FSD MRA in the frequency direction (craniocaudal axis) was 275.9 ± 29.7 mm. A total of 200 calf arterial segments were obtained, including 30 occlusive segments in 8 patients confirmed by CE MRA. After excluding 3 nondiagnostic segments with severe venous contamination in CE MRA, diagnostic agreement, sensitivity, specificity, PPV and NPV of FSD MRA were evaluated based on 197 segments, using CE MRA as a reference standard.

Image Quality

There was no significant difference detected in the rSI of arterial segments between FSD MRA and CE MRA (0.92 ± 0.09 versus 0.93 ± 0.05; P = 0.207) (Table 2).

Good intra-observer consistency acquired (kappa = 0.811, p<0.001) in image quality score assessment. The image quality score of FSD MRA was slightly higher than that of CE MRA (3.66 ± 0.81 versus 3.49 ± 0.87; P = 0.050) (Table 3). Venous contamination at the calf portion of CE MRA affected evaluation of infragenual arteries, which was found in 6 patients (6/20; 30.0%) affecting 39 arterial segments (39/200; 19.5%) (Figure 3). On per-patient's basis, no significant difference was observed in image quality assessment between CE and FSD MRA images (2.94 ± 1.06 for CE MRA vs 3.25 ± 1.06 for FSD MRA; P = 0.397).

After excluding the 30 occlusive segments, there was no difference in the number of diagnostic segments between the two techniques (FSD MRA (166/170, 97.6%) versus CE MRA (167/170, 98.2%), P = 0.319).

Diagnostic Performance

Good intra-observer consistency was acquired (kappa = 0.721, p<0.001) in arterial stenosis score assessment. Compared to CE MRA, the degree of stenosis was slightly overestimated by FSD MRA (2.19 ± 1.24 versus 2.09 ± 1.18; P = 0.019) (Table 4), with total agreement of 84.3% on the basis of all arterial segments (Table 5). An example case of overestimated stenosis using FSD is shown in Figure 4. On a segmental basis, the sensitivity, specificity, NPV, and PPV of FSD MRA for the detection of significant stenosis was 96.4%, 93.0%, 98.5%, and 84.1%, respectively (Table 5). On a per-patient basis, no significant difference in diagnostic performance was found between CE and FSD MRA images (3.27 ± 1.10 for CE MRA vs 3.27 ± 1.10 for FSD MRA; P = 1.000).

DSA

Six patients (30 arterial segments) in this study were evaluated by DSA examination. There was no significant difference in stenosis degree scores between MRA (FSD MRA and CE MRA) and DSA technique (2.47 ± 1.22 for FSD MRA, 2.47 ± 1.20 for CE MRA vs 2.40 ± 1.25 for DSA; P > 0.05) (Table 6). Compared with DSA, high agreement of MRA was detected (86.70% for FSD MRA, 93.30% for CE MRA). Using DSA images as reference, sensitivity, specificity, NPV, and PPV of FSD MRA for the detection of significant stenosis

was 100%, 94.1%, 100%, and 92.3%. On a per-patient basis, no significant difference in arterial stenosis assessment was found between MRA and DSA technique (3.50 ± 0.84 for FSD and CE MRA vs 3.83 ± 0.41 for DSA; P = 0.157).

DISCUSSION

The feasibility and diagnostic performance of FSD MRA on infragenual arteries at 3.0T were evaluated in this study. Compared to a prior 1.5T study (13), there was a similar diagnostic rate on the segment level with FSD MRA at 3.0T (98% versus 97.6%). Image quality and stenosis degree assessment using FSD MRA were assessed with CE MRA as the reference. FSD MRA provided diagnostic images allowing arterial stenosis assessment that was highly consistent with CE MRA. However, the agreement of bilateral anterior tibial arteries was lower compared to the other arteries. FSD MRA overestimated the lesions of bilateral anterior tibial arteries located at the curvature where arterial flow direction substantially changed. Studies of aortic arch coarctation demonstrated that moderate stenosis at the curvature of artery can provide complex downstream regional helix flow, vortex and recirculation (17,18). Elevated velocity was observed near coarctations for entire R-R interval, including diastolic phase. With similar geometry, elevated blood flow velocity during diastole near the lesions at curvature of bilateral anterior tibial arteries may have affected the bright-artery measurement.

In Liu's study (13), residual signal from soft tissues was more obvious in FSD MRA due to misregistration of two image sets acquired in a long scan time (4–5min). However in our study, FSD MRA had similar rSI values to CE MRA. We attribute this to the use of balanced SSFP. SNR efficient of balanced SSFP reduced the noise in the background soft tissues and provided excellent enhancement with arterial blood. Improved arterial blood enhancement can make the background residual signal inconspicuous.

Several noncontrast techniques have previously been used for lower extremities at 3.0T. Similar to FSD MRA, subtraction of datasets obtained during systole and diastole was achieved by using spin echo techniques. ECG-gated 3D half-Fourier TSE (nativeSPACE) sequence showed high susceptibility to motion, with nearly 50% of all cases non-diagnostic (19). In addition, the need for exact calibration of the trigger delay and flow-dephasing gradients in individual patients and vessel segments limited the diagnostic performance of the nativeSPACE technique, which can also affect FSD MRA. In this study, PC sequence was used to determine the blood flow profile above the bilateral popliteal trifurcations in order to choose the optimal systolic and diastolic phase for ECG triggering. ECG-gated quiescent-interval single-shot (QISS) with balanced SSFP performed at 3.0T in a previous study acquired credible angiographic images in the lower extremities (20–22). Nondiagnostic image quality occurred in some segments because of local field inhomogeneity (20). But shimming of the main magnetic field before each acquisition could obvious prolong the acquisition time (mean 18 min). Thus artifacts from patient motion during scan could result in degradation of image quality. Based on a 25-patient study (21), QISS MRA at the calf station showed similar image quality to CE MRA However, in our study image quality score was higher with FSD MRA. Furthermore, for detection of significant (>50%) stenosis, relative to CE MRA, sensitivity and specificity was 81.1% and

83.5% for QISS MRA, but higher for FSD MRA (96.4%, 93.0%) in this work. In a subgroup with 8 patients using DSA images as reference, sensitivity and specificity of QISS MRA was 100% and 76.5%, which was also improved for FSD MRA (100%, 94.1%) in this prior study.

Susceptibility to field inhomogeneity induced off-resonance artifacts have limited the wide use of SSFP sequence at 3.0T. In this study, manual field shimming was carefully performed to minimize frequency offset in the imaging volume. As a result, an adequate effective FOV in the frequency-encoding direction can be acquired to cover all the infragenual arteries. In order to further increase the effective FOV, a frequency scout could be used in future. The optimal offset frequency can be determined from a series of SSFP images acquired with several different offset frequencies. Thus, the artifacts can be moved out from the region of interest, though they cannot be fully avoided in all cases. Additionally, gradient echo (GRE) readout will be tested to perform FSD MRA to avoid known artifacts and SAR limitations of balanced SSFP at high field strengths (23).

Non-diagnostic FSD images were noted in 2 patients with occlusive lesion at bilateral superficial femoral arteries. A flat blood flow curve without obvious systolic phase was observed in the calf arteries. It is conjectured that occlusive lesions had affected the blood flow pattern in peripheral arteries. Systolic phase was delayed or even disappeared in distal arteries. In these cases, it was difficult to choose optimal systolic phase for the dark-artery scans (FSD preparation) at proximal and distal parts of occlusive segment simultaneously, as well as some patients with obvious different arterial stenosis degree at bilateral calve arteries. Thus slow downstream velocity for occlusive lesions might be the reason of the nondiagnostic image quality in FSD MRA. Notably, FSD MRA exhibited good performance on collateral arteries because of higher SNR and CNR, sensitivity of blood flow (13). Nevertheless, the performance of FSD MRA in occlusive lesions should be further studied.

Venous contamination degrades the image quality of CE MRA on lower extremity (24). In our study, CE MRA images in 6 patients exhibited obvious venous contamination. However, only 3 segments could not be evaluated. Other segments were diagnosed through rotating MIP images that avoided vein overlap. Using FSD MRA, venous contamination was considerably eliminated in calf arteries with excellent artery delineation. High consistency in diagnostic segments between FSD MRA and CE MRA was proved in our study. While time-resolved CE MRA was thought to be a good method to solve the venous contamination problem in the calf, additional contrast medium administration is required. Additionally spatial resolution has to be traded to ensure sufficient temporal resolution to avoid venous contamination. Using the FSD MRA technique can benefit patients from avoiding adverse events associated with contrast media.

We chose CE MRA as the reference standard, which may lead to bias of the stenosis evaluation accuracy. DSA should be the best reference standard. But DSA procedure is less commonly performed due to its invasiveness and ionizing radiation. CE MRA is deemed as an accurate alternative and commonly used for evaluating peripheral artery disease. For these reasons, we have limited the scope of our work to investigating whether FSD MRA at 3.0T could still offer comparable diagnostic value when comparing to CE MRA. On the

other hand, we have included 6 patients who underwent interventional revascularization where DSA could be conducted. There was no significant difference in stenosis degree scores between CE MRA and DSA technique. Nevertheless, future studies on comparison with DSA are warranted to fully establish the clinical usefulness of FSD-MRA. Otherwise, the number of cases in this study was limited.

Iliac and femoral arteries were not included in the study, because of the limit of prolonged scan time. Compared to iliac and femoral arteries, calf arteries were more difficult to perform non-contrast MRA with branch vessels in different orientations. Furthermore, there is need for non-contrast alternative in this region to address venous contamination in the CE MRA method. Thus, we chose infragenual arteries for the position underwent FSD MRA. Iliac and femoral arteries will be studied in separate studies in the future.

In conclusion, FSD MRA of infragenual can be performed at 3.0T with diagnostic image quality without contrast agent. It is shown to have good diagnostic performance on arterial stenosis degree assessment with CE MRA as the reference standard.

Acknowledgments

None.

Grant Support:

This research was supported by the Beijing Natural Science Foundation (grant 7132086), National Institutes of Health of USA (Grant Number 1R01HL096119), and American Heart Associate (Grant Number AHA11POST7650043).

References

1. Fowkes FGR, Rudan D, Rudan I, et al. Comparison of global estimates of prevalence and risk factors for peripheral artery disease in 2000 and 2010: a systematic review and analysis. The Lancet. 2013; 382(9901):1329–1340.
2. Hirsch AT, Haskal ZJ, Hertzer NR, et al. ACC/AHA Guidelines for the Management of Patients with Peripheral Arterial Disease (lower extremity, renal, mesenteric, and abdominal aortic): a collaborative report from the American Associations for Vascular Surgery/Society for Vascular Surgery, Society for Cardiovascular Angiography and Interventions, Society for Vascular Medicine and Biology, Society of Interventional Radiology, and the ACC/AHA Task Force on Practice Guidelines (writing committee to develop guidelines for the management of patients with peripheral arterial disease)–summary of recommendations. Journal of vascular and interventional radiology : JVIR. 2006; 17(9):1383–1397. quiz 1398. [PubMed: 16990459]
3. Thomsen HS. Nephrogenic systemic fibrosis: A serious late adverse reaction to gadodiamide. European radiology. 2006; 16(12):2619–2621. [PubMed: 17061066]
4. Marckmann P, Skov L, Rossen K, et al. Nephrogenic systemic fibrosis: suspected causative role of gadodiamide used for contrast-enhanced magnetic resonance imaging. Journal of the American Society of Nephrology : JASN. 2006; 17(9):2359–2362. [PubMed: 16885403]
5. Miyazaki M, Lee VS. Nonenhanced MR angiography. Radiology. 2008; 248(1):20–43. [PubMed: 18566168]
6. Miyazaki M, Sugiura S, Tateishi F, Wada H, Kassai Y, Abe H. Non-contrast-enhanced MR angiography using 3D ECG-synchronized half-Fourier fast spin echo. Journal of magnetic resonance imaging : JMRI. 2000; 12(5):776–783. [PubMed: 11050650]
7. Edelman RR, Sheehan JJ, Dunkle E, Schindler N, Carr J, Koktzoglou I. Quiescent-interval single-shot unenhanced magnetic resonance angiography of peripheral vascular disease: Technical considerations and clinical feasibility. Magnetic resonance in medicine : official journal of the

Society of Magnetic Resonance in Medicine / Society of Magnetic Resonance in Medicine. 2010; 63(4):951–958.

8. Edelman RR, Giri S, Murphy IG, Flanagan O, Speier P, Koktzoglou I. Ungated radial quiescent-inflow single-shot (UnQISS) magnetic resonance angiography using optimized azimuthal equidistant projections. Magnetic resonance in medicine : official journal of the Society of Magnetic Resonance in Medicine / Society of Magnetic Resonance in Medicine. 2014; 72(6):1522–1529.
9. Fan Z, Sheehan J, Bi X, Liu X, Carr J, Li D. 3D noncontrast MR angiography of the distal lower extremities using flow-sensitive dephasing (FSD)-prepared balanced SSFP. Magnetic resonance in medicine : official journal of the Society of Magnetic Resonance in Medicine / Society of Magnetic Resonance in Medicine. 2009; 62(6):1523–1532.
10. Wedeen VJ, Meuli RA, Edelman RR, et al. Projective imaging of pulsatile flow with magnetic resonance. Science. 1985; 230(4728):946–948. [PubMed: 4059917]
11. Meuli RA, Wedeen VJ, Geller SC, et al. MR gated subtraction angiography: evaluation of lower extremities. Radiology. 1986; 159(2):411–418. [PubMed: 3961174]
12. Lim RP, Fan Z, Chatterji M, et al. Comparison of nonenhanced MR angiographic subtraction techniques for infragenual arteries at 1.5 T: a preliminary study. Radiology. 2013; 267(1):293–304. [PubMed: 23297320]
13. Liu X, Zhang N, Fan Z, et al. Detection of infragenual arterial disease using non-contrast-enhanced MR angiography in patients with diabetes. Journal of magnetic resonance imaging : JMRI. 2014; 40(6):1422–1429. [PubMed: 24925770]
14. Liu X, Fan Z, Zhang N, et al. Unenhanced MR angiography of the foot: initial experience of using flow-sensitive dephasing-prepared steady-state free precession in patients with diabetes. Radiology. 2014; 272(3):885–894. [PubMed: 24758556]
15. Fan Z, Zhou X, Bi X, Dharmakumar R, Carr JC, Li D. Determination of the optimal first-order gradient moment for flow-sensitive dephasing magnetization-prepared 3D noncontrast MR angiography. Magnetic resonance in medicine : official journal of the Society of Magnetic Resonance in Medicine / Society of Magnetic Resonance in Medicine. 2011; 65(4):964–972.
16. Asbach P, Meade MD, Sattenberg RJ, Klessen C, Huppertz A, Heidenreich JO. Continuously moving table aorto-iliofemoral run-off contrast-enhanced magnetic resonance angiography: image quality analysis in comparison to the multistep acquisition. Acta radiologica. 2014; 55(3):266–272. [PubMed: 24078458]
17. Frydrychowicz A, Markl M, Hirtler D, et al. Aortic hemodynamics in patients with and without repair of aortic coarctation: in vivo analysis by 4D flow-sensitive magnetic resonance imaging. Investigative radiology. 2011; 46(5):317–325. [PubMed: 21285892]
18. LaDisa JF Jr, Alberto Figueroa C, Vignon-Clementel IE, et al. Computational simulations for aortic coarctation: representative results from a sampling of patients. Journal of biomechanical engineering. 2011; 133(9):091008. [PubMed: 22010743]
19. Haneder S, Attenberger UI, Riffel P, Henzler T, Schoenberg SO, Michaely HJ. Magnetic resonance angiography (MRA) of the calf station at 3.0 T: intraindividual comparison of non-enhanced ECG-gated flow-dependent MRA, continuous table movement MRA and time-resolved MRA. European radiology. 2011; 21(7):1452–1461. [PubMed: 21274715]
20. Knobloch G, Gielen M, Lauff MT, et al. ECG-gated quiescent-interval single-shot MR angiography of the lower extremities: initial experience at 3 T. Clinical radiology. 2014; 69(5): 485–491. [PubMed: 24613581]
21. Hansmann J, Morelli JN, Michaely HJ, et al. Nonenhanced ECG-gated quiescent-interval single shot MRA: image quality and stenosis assessment at 3 tesla compared with contrast-enhanced MRA and digital subtraction angiography. Journal of magnetic resonance imaging : JMRI. 2014; 39(6):1486–1493. [PubMed: 24338813]
22. Thierfelder KM, Meimarakis G, Nikolaou K, et al. Non-contrast-enhanced MR angiography at 3 Tesla in patients with advanced peripheral arterial occlusive disease. PloS one. 2014; 9(3):e91078. [PubMed: 24608937]
23. Johst S, Orzada S, Fischer A, et al. Sequence comparison for non-enhanced MRA of the lower extremity arteries at 7 Tesla. PloS one. 2014; 9(1):e86274. [PubMed: 24454963]

24. Riffel P, Haneder S, Attenberger UI, Brade J, Schoenberg SO, Michaely HJ. Combined large field-of-view MRA and time-resolved MRA of the lower extremities: impact of acquisition order on image quality. European journal of radiology. 2012; 81(10):2754–2758. [PubMed: 22185939]

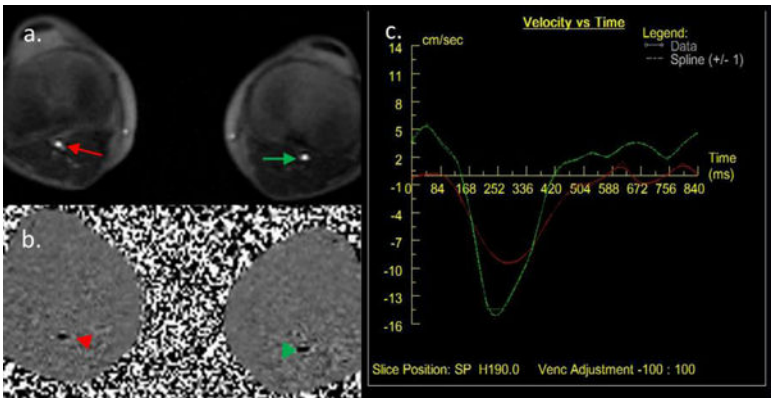

Figure 1.

Detection of the systolic and diastolic phase for ECG trigger with PC sequence. a. cine image of bilateral popliteal arteries (arrow); b. phase image of bilateral popliteal arteries (arrowhead); c. blood flow velocity curve through R-R interval of bilateral popliteal arteries. (Red, right popliteal artery; Green, left popliteal artery)

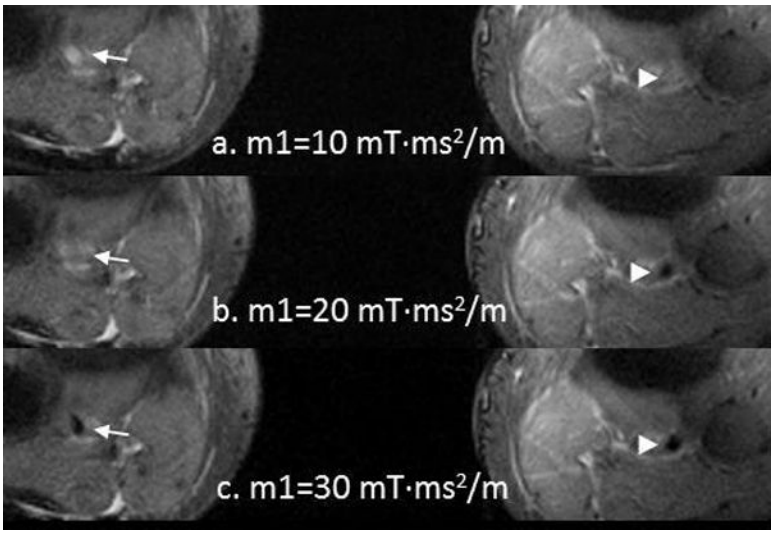

Figure 2.

First-order gradient moment (m1) scouts for bilateral popliteal arteries. a. m1=10 $mT \cdot ms^2/m$, bright blood in bilateral popliteal arteries lumen; b. m1=20 $mT \cdot ms^2/m$, bright blood in right popliteal artery lumen (arrow), and dark blood in left one (arrowhead); c. m1=30 $mT \cdot ms^2/m$, dark blood in bilateral popliteal arteries lumen. In this case, the optimal M1 was 30 $mT \cdot ms^2/m$.

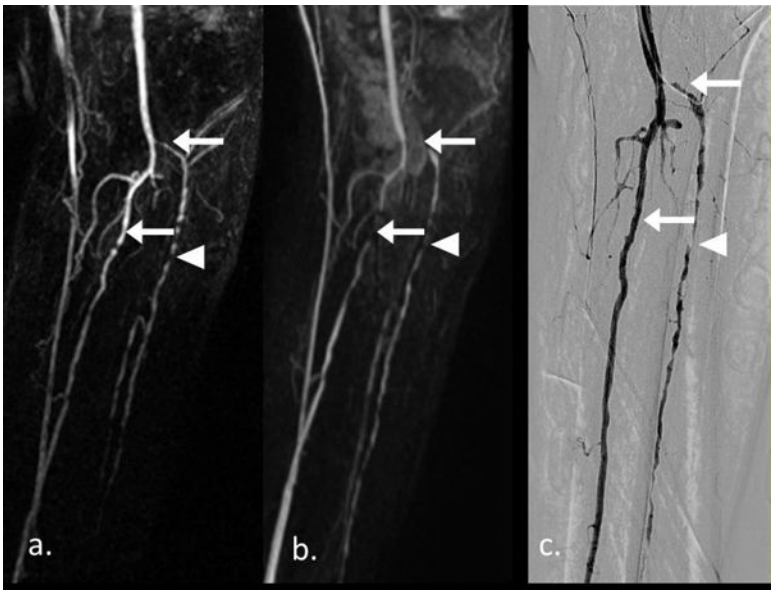

Figure 3.

A 83-years-old male patient with a 2 years history of intermittent claudication, and left little toe gangrene for 1 month. Left perennial artery occluded in FSD MRA (a) with confirmation of CE MRA and DSA (b & c). And multiple arterial stenosis lesions in left anterior tibial artery with different degree were shown in three techniques (arrowhead). Venous contamination overlapped left anterior tibial artery and posterior tibial artery (arrow). Useful FOV on frequency direction was 325.2 mm.

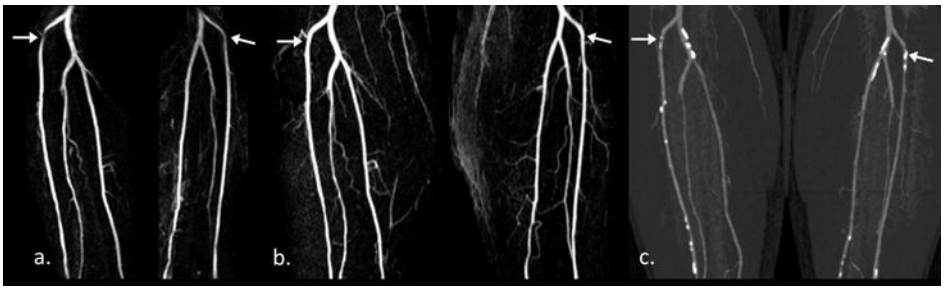

Figure 4.

A 61-years-old male patient with diffused arthrosclerosis. Compared with CE MRA (b), overestimated stenosis lesions (arrow) at bilateral anterior tibial artery were shown on FSD MRA (a). From CTA images (c), multiple calcified plaques can be noticed there. Useful FOV on frequency direction was 266.2 mm.

Table 1

Patients' Characteristics

Characteristics[a]	Value
Age (mean/range)	59.61±18.25 / 14–84 years
Sex (male/female)	15 / 5
BMI (kg·m^{-2})	25.75±3.99
Smoke	17 (85.0)
SBP (mmHg)	127.00±20.02
DBP (mmHg)	84.00±13.93
Hypertension	7 (35.0)
Intermittent claudication	16 (80.0)
Rest pain	4 (20.0)
Gangrene	3(15.0)
Acute thrombosis	2 (10.0)

[a]Continuous data are presented as mean ± standard deviation and categoric data as number (%).

BMI = Body mass index; SBP = Systolic blood pressure; DBP = Diastolic blood pressure.

Table 2

rSI of Bilateral Calf Arterial Segments

	Segments[a]	FSD MRA	CE MRA	t	P Value
Right Calf	Popliteal Artery	0.92±0.08	0.92±0.05	.360	.724
	Tibioperoneal trunk	0.91±0.10	0.94±0.03	−.499	.625
	Anterior Tibial Artery	0.91±0.10	0.94±0.03	−.848	.410
	Posterior Tibial Artery	0.92±0.11	0.92±0.05	.183	.857
	Perennial artery	0.96±0.03	0.93±0.05	1.131	.276
Left Calf	Popliteal Artery	0.90±0.11	0.94±0.08	−1.031	.319
	Tibioperoneal trunk	0.91±0.08	0.95±0.03	−1.996	.064
	Anterior Tibial Artery	0.91±0.09	0.93±0.07	−.740	.471
	Posterior Tibial Artery	0.91±0.11	0.91±0.06	−2.19	.830
	Perennial artery	0.93±0.09	0.91±0.05	.306	.764
Total		0.92±0.09	0.93±0.05	−1.266	.207

[a]Continuous data are presented as mean ± standard deviation.

rSI = Relative signal intensity

Table 3

Image Quality Scores of Bilateral Calf Arterial Segments

	Segments[a]	FSD MRA	CE MRA	Z	P Value
Right Calf	Popliteal Artery	3.87±0.52	3.73±0.59	−0.557	.577
	Tibioperoneal trunk	3.85±0.55	3.61±0.77	−0.756	.450
	Anterior Tibial Artery	3.69±0.85	3.38±1.04	−0.816	.414
	Posterior Tibial Artery	3.67±0.89	3.67±0.78	−0.000	1.000
	Perennial artery	4.00±0.00	3.45±0.93	−1.732	.083
Left Calf	Popliteal Artery	3.38±1.02	3.69±0.60	−0.997	.319
	Tibioperoneal trunk	3.67±0.62	3.33±0.98	−1.186	.236
	Anterior Tibial Artery	3.50±0.94	3.29±1.07	−0.744	.457
	Posterior Tibial Artery	3.71±0.73	3.57±0.76	−0.552	.581
	Perennial artery	3.19±1.42	2.94±1.34	−0.954	.340
Total		3.66±0.81	3.49±0.87	−1.960	.050

[a]Continuous data are presented as mean ± standard deviation.

Table 4

Stenosis Degree Scores of Bilateral Calf Arterial Segments

Segments[a]		FSD MRA	CE MRA	Z	P Value
Right Calf	Popliteal Artery	1.56±1.03	1.63±1.09	−1.000	.317
	Tibioperoneal trunk	2.25±1.18	2.19±1.17	−1.000	.317
	Anterior Tibial Artery	2.69±1.25	2.56±1.37	−0.707	.480
	Posterior Tibial Artery	2.44±1.37	2.38±1.36	−0.447	.655
	Perennial artery	2.50±1.32	2.44±1.15	−0.378	.705
Left Calf	Popliteal Artery	1.44±0.89	1.25±0.58	−0.816	.414
	Tibioperoneal trunk	1.88±1.09	1.75±0.93	−1.000	.317
	Anterior Tibial Artery	2.63±1.31	2.50±1.16	−0.707	.480
	Posterior Tibial Artery	2.25±1.29	2.19±1.22	−1.000	.317
	Perennial artery	2.31±1.25	2.00±1.16	−1.890	.059
Total		2.19±1.24	2.09±1.18	−2.340	.019

[a]Continuous data are presented as mean ± standard deviation.

Table 5

Diagnostic Efficiency of FSD MRA (Compared with CE MRA)

Segments		Agreement	Sensitivity	Specificity	NPV	PPV
Right Calf	Popliteal Artery	95.0%	66.7%	100.0%	94.4%	100.0%
	Tibioperoneal trunk	95.0%	100.0%	92.9%	100.0%	85.7%
	Anterior Tibial Artery	73.7%	87.5%	90.9%	90.9%	87.5%
	Posterior Tibial Artery	90.0%	100.0%	91.7%	100.0%	88.9%
	Perennial artery	80.0%	100.0%	84.6%	100.0%	77.8%
Left Calf	Popliteal Artery	85.0%	100.0%	89.5%	100.0%	33.3%
	Tibioperoneal trunk	78.9%	100.0%	94.1%	100.0%	66.7%
	Anterior Tibial Artery	57.9%	100.0%	91.7%	100.0%	87.5%
	Posterior Tibial Artery	95.0%	100.0%	100.0%	100.0%	100.0%
	Perennial artery	80.0%	100.0%	92.9%	100.0%	85.7%
Total		84.3%	96.4%	93.0%	98.5%	84.1%

Table 6

Diagnostic Efficiency of MRA (Compared with DSA)

Sequences	Stenosis Degree Scores	DSA	P	Agreement	Sensitivity	Specificity	NPV	PPV
FSD MRA	2.47 ± 1.22	2.40 ± 1.25	.317	86.7%	100%	94.1%	100%	92.3%
CE MRA	2.47 ± 1.20		.157	93.3%	100%	100%	100%	100%

[a]Continuous data are presented as mean ± standard deviation.